University of Szeged

Faculty of Pharmacy

Department of Pharmacodynamics and Biopharmacy

Antiproliferative and Antimetastatic Properties of A- or D-ring Modified Estrone Analogs

Summary of Ph.D. Thesis

Seyyed Ashkan Senobar Tahaei

Szeged

2023

University of Szeged, Faculty of Pharmacy
Doctoral School of Pharmaceutical Sciences

Educational program: Pharmacodynamics, Biopharmacy and Clinical Pharmacy

Head of the program: Prof. Dr. István Zupkó D.Sc.

DEPARTMENT OF PHARMACODYNAMICS AND BIOPHARMACY

SUPERVISOR: Prof. Dr. István Zupkó D.Sc.

Seyyed Ashkan Senobar Tahaei Pharm.D.

Antiproliferative and Antimetastatic Properties of A- or D-ring Modified Estrone Analogs

Complex Exam Committee:

Head: Prof. Dr. Gyöngyvér Soós Ph.D.

Members: Dr. Anna Borsodi D.Sc.

Dr. Ducza Eszter Ph.D.

Reviewers Committee:

Head: Prof. Dr. István Ilisz, D.Sc.

Reviewers: Dr. István Lekli, Ph.D.

Dr. Gabriella Spengler, Ph.D.

Member: Dr. Szilvia Berkó, Ph.D.

Secretary: Dr. Tivadar Kiss, Ph.D.

1. Introduction

Cancer has emerged as a substantial global contributor to mortality, with its impact comparable to that of stroke and coronary heart disease. The International Agency for Research on Cancer (IARC) database's update for 2020 revealed a stark reality: 19.3 million new cancer cases and nearly 10 million related deaths globally. This trend is projected to intensify, with an anticipated surge in cancer incidence to 28.4 million cases by 2040, underscoring the urgency of resource allocation for effective prevention, early detection, and comprehensive treatment strategies. Among the distressing statistics, lung cancer ranks as the leading cause of cancer-related deaths, followed by colorectal, liver, stomach, and breast cancers. These numbers accentuate the need for advanced research, diagnostic tools, and innovative treatments.

Focusing on demographics, breast cancer dominates new diagnoses among females, accounting for a concerning 24.5% of cases. Addressing this requires heightened awareness campaigns, accessible screenings, and research to bolster early interventions. Moreover, gynecological malignancies attribute 38.9% of new female cancer cases, spotlighting cancer's complex nature and the need for comprehensive strategies. Collaborative efforts across researchers, medical professionals, policymakers, and communities are vital to mitigate the escalating cancer burden. Furthermore, the regional distribution of the 2.26 million female breast cancer cases in 2020 highlights disparities across geographical areas. Incidence rates vary, from Europe's 69.7 cases per 100,000 individuals to South-East Asia's 28.3. Notably, a correlation between the mortality-to-incidence ratio (MIR) and the human development index (HDI) underscores an inverse relationship, indicating that less developed regions experience higher MIRs. This connection emphasizes the challenge faced by patients in underdeveloped areas with limited access to advanced healthcare and comprehensive treatments. Addressing these disparities demands a global effort that acknowledges the intricate links between healthcare access, socio-economic development, and cancer outcomes. Despite therapeutic advancements, the epidemiological data reiterate the ongoing challenges in breast cancer prevention and treatment.

Steroids, a group of compounds with diverse roles, hold promise in combating cancer. Elevated steroid receptor expression in hormone-dependent tumors, like those in

breast, uterine, ovarian, prostate, and endometrial contexts, boosts cell proliferation. Strategies targeting hormone-induced growth response have been explored. Globally, 2020 has recorded 19.3 million new cancer cases and almost 10 million cancer-related deaths, projected to rise to 28.4 million by 2040. Breakthroughs like cyproterone, finasteride, exemestane, and fulvestrant have transformed cancer treatment, with exemestane showing efficacy against postmenopausal breast cancer. Steroidal compounds with cytotoxic attributes affect molecular targets like microtubules and topoisomerases, halting cell cycles and triggering apoptosis. Steroid compounds from nature or synthesis are gaining attention for their efficacy against cancer cells through non-hormonal pathways. However, developing innovative drug candidates involves modifying natural molecules to create semi-synthetic analogs with tailored properties. Triterpenes like betulinic and oleanolic acids exhibit promising anti-cancer properties. Recent research explores modifications to estrane-based compounds, unveiling potential agents against cancer. Tailored core-modified estrones engage with cellular processes and disrupt tubulin-microtubule interactions, hindering cell division. Recent findings highlight the potential of 16,17-functionalized 3-methoxy or 3-benzyloxy estrone derivatives as potent antiproliferative compounds. The study aims to assess the antiproliferative and antimetastatic properties of novel 16-azidomethyl-17-hydroxy and 17-keto derivatives.

the objective of this study is to assess the antiproliferative, antimetastatic, and anticancer properties of 17-keto compounds **16AABE** and **16BABE** (Figure 1)

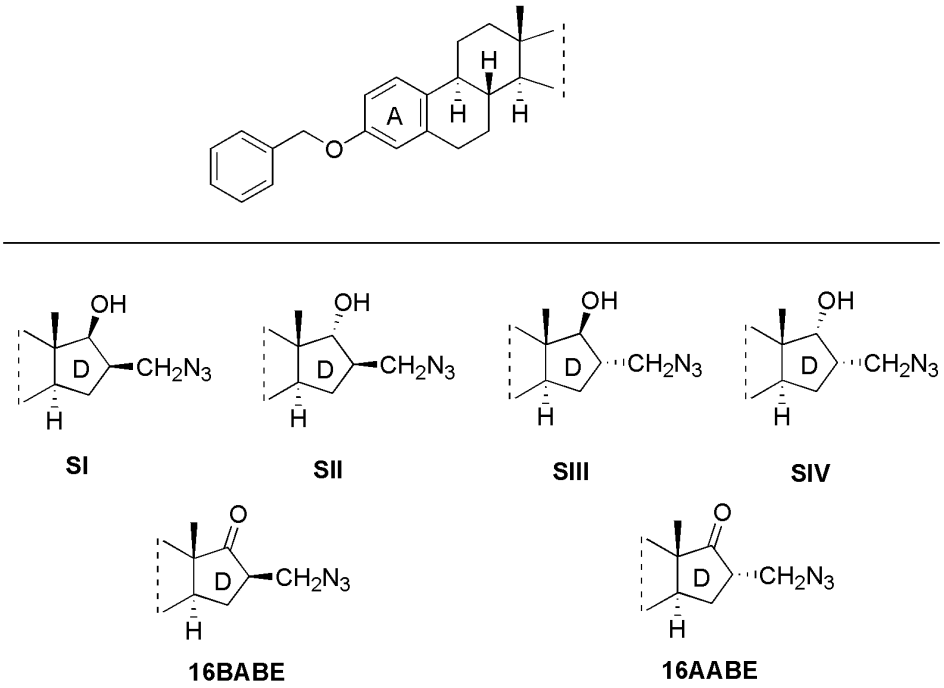

Figure 1. Structures of the tested starting compounds (SI–SIV) and the newly synthesized 16β-azidomethyl-3-O-benzyl estrone (16BABE) and 16α-azidomethyl-3-O-benzyl estrone (16AABE).

2. Aims of The Study

The primary aim of this study was to explore the potential antiproliferative and antimetastatic characteristics of these promising compounds. This investigation was conducted through in vitro experiments on cell lines associated with breast and gynecological tumors. Additionally, the study aimed to uncover the underlying mechanism that drives these compound's actions, providing insights into their mode of operation.

The performed experiments aimed to achieve the following objectives:

- The experiments are designed to elucidate the antiproliferative properties of the tested compounds on breast and gynecological cancer cell lines. Furthermore, the IC_{50} values of these compounds are being ascertained utilizing the established MTT assay protocol.

- The study encompasses the estimation of tumor selectivity indices across all examined cell lines, with a comparative reference to a non-cancerous cell line (NIH/3T3).

- In this study, the objective of performing the PI staining cell cycle by flow cytometry was to investigate the distribution of cells within different phases of the cell cycle. This method allows for a comprehensive understanding of cellular progression, aiding in assessing potential alterations induced by the experimental conditions and providing valuable insights into the mechanistic underpinnings of the observed effects.

- Conducting the tubulin polymerization assay serves as a method to evaluate the influence of the tested compounds on tubulin dynamics. This assay offers valuable insights into the potential implications for cell growth and migration, which are pivotal for comprehending their therapeutic prospects, particularly within cancer research.

- This investigation aims to assess the tested compound's inhibitory impacts on the initial stages of metastasis development, including migration and invasion. This objective will be achieved through the implementation of wound-healing and Boyden chamber assays, which collectively offer insights into the compound's potential to hinder these critical processes.

- Measuring the estrogenic activity of the test compounds using a transfected cell line provides valuable insights into the hormonal properties of the tested molecules.

3. Materials and Methods

3.1. Cell Culture and Chemicals

In this study compounds were tested against HeLa, MDA-MB-231, MCF-7, A2780, SiHa, T47D-KBluc and NIH/3T3 cells. All cell lines were cultured in Eagle's Minimum Essential Medium (EMEM) at 37 °C in a humidified atmosphere with 5% carbon dioxide. The medium was supplemented with 10% fetal bovine serum (FBS), 1% non-essential amino acid solution, and 1% penicillin, streptomycin, and amphotericin B mixture.

3.2. Determination of Antiproliferative Activity (MTT Assay)

Cancer cells were seeded in a 96-well microplate for the proliferation assay at 5000 cells/well density. After 24 hours of incubation, 200 µL of new medium containing the tested compounds at 10 or 30 μM concentrations was added. Following incubation for 72 hours at 37 °C in a humidified atmosphere containing 5% CO_2, cell viability was assessed by adding 20 µL of a 5 mg/ml 3-(4,5-dimethylthiazol-2-yl)-2,5-diphenyltetrazolium bromide (MTT) solution. The yellow MTT solution was converted to violet crystals by mitochondrial reductases in viable cells after a 4-hour incubation. Subsequently, the medium was removed, and the formazan crystals were dissolved in 100 µL of DMSO with shaking at 37 °C for 60 minutes. The absorbance of the reduced MTT solution was measured at 545 nm using a microplate reader, with untreated cells serving as the negative control. In the case of active compounds (i.e., higher than 50% cell growth inhibition at 10 or 30 µM), the assay was repeated with a series of dilutions, and sigmoidal dose-response curves were fitted to the obtained data. The IC_{50} values, representing the concentration at which cell proliferation was reduced by 50% compared to the untreated control, were calculated using GraphPad Prism 5. Each in vitro experiment was conducted on two microplates with a minimum of five parallel wells. Stock solutions of the tested substances (10 mM) were prepared in DMSO, with the highest DMSO concentration in the medium not exceeding 0.3%, which did not significantly affect cell proliferation. Cisplatin was used as the reference agent.

3.3. Propidium Iodide-based Cell Cycle Analysis

Cell cycle analysis was conducted to investigate the mechanism of action of azidomethyl compounds in human breast cancer cell lines. Specifically, MDA-MB-231 cells were seeded in 24-well plates at a density of 80,000 cells per well. The cells were treated with six concentrations of **16AABE** (0.5, 1 and 2 µM) and **16BABE** (2, 4 and 8

μM) for 24 hours. After treatment, the cells were washed with phosphate-buffered saline (PBS) and harvested using trypsin. The harvested cells were combined with the supernatants and PBS from the washing process. Subsequently, centrifugation at 1,700 rpm for 5 minutes at room temperature was performed, followed by resuspending the cell pellets in a DNA staining solution. The DNA staining solution consisted of 10 μg/mL propidium iodide (PI), 0.1% Triton-X, 10 μg/mL RNase A, and 0.1% sodium citrate dissolved in PBS. The resuspended cells were then incubated in the dark at room temperature for 30 minutes. At least 20,000 events per sample were analyzed using a FACSCalibur flow cytometer to assess the DNA content. The data obtained were analyzed using ModFit LT 3.3.11 software. Untreated cells were the control, and a hypodiploid (subG1) phase indicated the apoptotic cell population.

3.4. Tubuline Polimerization Assay

Following the manufacturer's instructions, a tubulin polymerization assay kit was employed to assess the cell-independent direct effects of test compounds on tubulin polymerization in vitro. Initially, 10 μL of a 500 μM solution of the desired compound was added to a UV-transparent microplate prewarmed to 37°C. Positive control samples containing 10 μL of 10 μM paclitaxel and untreated controls with general tubulin buffer were also prepared. Next, 100 μL of a 3.0 mg/mL tubulin solution dissolved in polymerization buffer was added to each sample well in separate wells of a 96-well plate. The plate was immediately placed in an ultraviolet spectrophotometer prewarmed to 37°C. A 60-minute kinetic reaction was initiated, during which the absorbance was measured at 340 nm every minute to evaluate the effects of the tested compounds. The tubulin polymerization curve was constructed by plotting the optical density against time. The maximum reaction rate (Vmax; Δabsorbance/min) was calculated based on the highest difference in absorbance observed over three consecutive time points on the kinetic curve.

3.5. Migration Assay

As previously described, MCF-7 cell suspension was prepared in a supplemented EMEM. The cells were then seeded onto 12-well plates using specialized Ibidi silicone inserts at a concentration of 25,000 cells per well. The silicone inserts were gently removed after overnight incubation, and the cells were washed with PBS. Subsequently, the cells were subjected to a wound healing assay by treating them with low concentrations of compounds (1.5 and 3 μM) prepared in EMEM medium with reduced serum content (2% FBS). The antimigratory effect of the compounds was

assessed by measuring the size of the cell-free areas. Images of the cell monolayer were captured at 0, 24, and 48 hours using the QCapture Pro software. Based on the captured images, the size of the cell-free areas was determined using the ImageJ software.

3.6. Invasion Assay

To assess the impact of our compounds on the invasion capacity of malignant MDA-MB-231 cells, we employed Boyden chambers equipped with a reconstituted membrane that mimics the basement membrane. The treated cells were carefully pipetted onto the hydrated membranes in the upper chamber. In the lower chamber, EMEM supplemented with 10% FBS served as a chemoattractant. After a 24-hour incubation period, the supernatants were removed, and non-invading cells on the upper side of the membrane were gently wiped away using a cotton swab. The membrane was then rinsed twice with PBS and fixed with ice-cold 96% ethanol. Subsequently, invading cells were stained with a 1% crystal violet dye solution for 30 minutes in the dark at room temperature. Multiple images (at least three per insert) were captured using a Nikon Eclipse TS100 microscope. Finally, the invading cells were quantified and compared to untreated control samples.

3.7. Determination of Estrogenic Activity

T47D human breast adenocarcinoma cells expressing endogenous estrogen receptor (ERα) modified with an estrogen-responsive luciferase (Luc) reporter gene (T47D-KBluc) were used to assess the estrogenic activity of tested compounds. Cells were maintained in phenol red-free MEM with 2 mM L-glutamine, 1 g/L glucose, 10% FBS and penicillin-streptomycin antibiotics. Before testing the compound's effect, cells were maintained in the same medium above but supplemented with 10% charcoal dextran-treated FBS for at least six days. Cells were seeded at a density of 50,000 per well in 200 μl of the medium above in a 96-well white flat bottom plate and allowed to attach for 72 h. Then the indicated concentrations of the test compounds and the reference agent 17β-estradiol were added. Plates were incubated at 37°C in a humidified 5% CO_2 incubator before measuring luciferase activity. After 24 h incubation, the dosing media was removed entirely, and 30 µl of One-Glo firefly luciferase reagent per well was added to the plate and then incubated for 3 minutes at room temperature according to the manufacturer protocol and the luminescence signal was quantified.

3.8. Statistical Analysis

The statistical analysis of the obtained results was conducted using the GraphPad Prism 5 software. One-way analysis of variance (ANOVA) was employed, followed by the Dunnett posttest, to assess the significance of the observed differences. Data are expressed as mean values ± standard error of the mean (SEM).

4. Results

4.1. Antriproliferative Activity

As described above, 3 set of compounds were screened by standard MTT-assay. The results have been compared each other according to structure–activity relationships and growth inhibition percentage. Our goal was to find most effective compounds against cancer cell lines based on sensitivity to the cell line. Only two potential compounds (**16AABE** and **16BABE**) were selected. The investigation of tumor selectivity in intact human fibroblast cell lines revealed that the selectivity of the test compounds for the cancerous cells are comparable with reference agent (cisplatin).

Table 1. Growth Inhibition, % ± SEM and IC50 values of 16AABE and 16BABE

Cell line		Conc. (μM)	**16 AABE**	**16 BABE**	Cisplatin*
HeLa	Inhibition %	10 μM	93.40±0.13	93.22±0.92	42.61 ± 2.33
		30 μM	94.33±0.32	93.96±0.23	99.93 ± 0.26
	Calculated IC_{50} (μM)		[4.60]	[5.01]	[12.43]
SiHa	Inhibition %	10 μM	90.73±0.53	90.10±0.66	86.84 ± 0.50
		30 μM	91.08±0.55	91.48±0.55	90.18 ± 1.78
	Calculated IC_{50} (μM)		[3.85]	[4.10]	[7.84]
MCF-7	Inhibition %	10 μM	92.94±0.37	91.73±0.71	53.03 ± 2.29
		30 μM	93.79±0.40	93.85±0.22	86.90 ± 1.24
	Calculated IC_{50} (μM)		[3.15]	[3.13]	[5.78]
MDA-MB-231	Inhibition %	10 μM	93.65±0.24	93.35±0.17	20.84 ± 0.81
		30 μM	95.03±0.23	95.11±0.31	74.47 ± 1.20
	Calculated IC_{50} (μM)		[8.13]	[4.72]	[19.13]
NIH 3T3	Inhibition %	10 μM	<20	<20	94.20 ± 0.39
		30 μM	94.79	98.29	96.44 ± 0.17
	Calculated IC_{50} (μM)		[18.93]	[13.59]	[3.23]

Table 2. Tumor selectivity indices of 16AABE and 16BABE expressed as the ratio of IC50 values obtained against cancer cells and fibroblasts.

Cancer cell line	$\frac{IC_{50} \text{ of cancer cell line}}{IC_{50} \text{ of NIH/3T3}}$	
	16AABE	**16BABE**
HeLa	0.369	0.243
SiHa	0.302	0.203
MCF-7	0.230	0.166
MDA-MB-231	0.347	0.429

4.2. Propidium Iodide-based Cell Cycle Analysis

Test compounds were subjected to propidium iodide-based cell cycle analysis by flow cytometry. MDA-MB-231 cells were treated with various concentrations for 24 hours. **16AABE** resulted in a moderate but significant increase in the hypodiploid (subG1) population at 1 μM (Figure 2). At 2 μM, which is approximately the IC_{50} value, a more profound cell cycle disturbance was observed with a pronounced increase of subG1 and G2/M populations at the expense of G1 and S phases. **16BABE**, conversely, caused a minor but significant accumulation of subG1 cells at 8 μM, a concentration roughly its IC_{50}, indicating the proapoptotic activity of the compound (Figure 2).

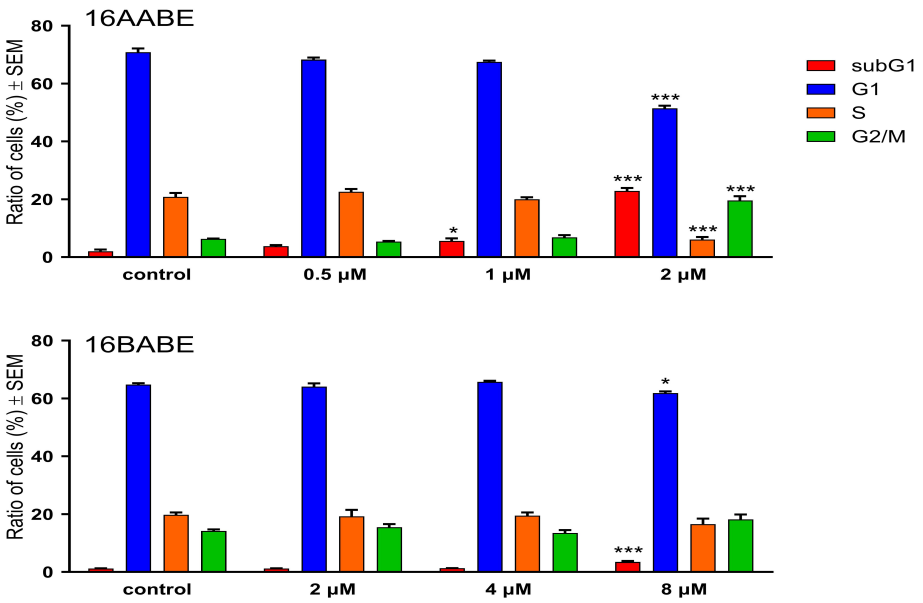

*Figure 2. Effects of 16AABE (upper panel) and 16BABE (lower panel) on cell cycle distribution of MDA-MB-231 cells treated with the indicated concentrations for 24 hours. * and *** indicate significant differences at p<0.05 and p<0.001, respectively. Data are from three independent experiments performed in triplicate.*

4.3. Tubulin Polymerization Assay

The impact of the test compounds on microtubule polymerization was assessed using a cell-free system with a photometric kinetic determination. The concentrations of the test compounds were selected based on their IC_{50} values, as the kit's manufacturer recommended. Notably, the calculated maximum tubulin polymerization (Vmax) rates were significantly higher than those observed in the control condition (Figure 3). It is worth mentioning that the Vmax values of the tested compounds were higher than that of the reference agent paclitaxel (PAC, 10 μM), indicating their profound activity on the polymerization of tubulin.

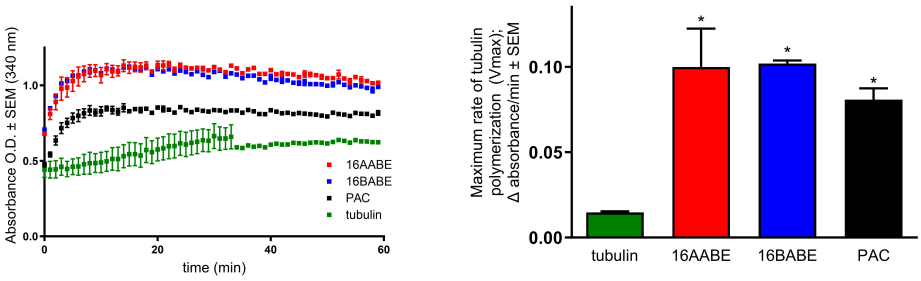

*Figure 3. Direct effects of 16AABE and 16BABE (500 μM for both) on tubulin polymerization. Left panel: recorded kinetic curves; paclitaxel (10 μM PAC) was included as a reference agent. Right panel: calculated maximum values for the rate of tubulin polymerization. * Indicate significance at p<0.05 compared to untreated tubulin – results from two independent experiments performed in duplicate.*

4.4. Wound Healing Assay

To investigate the antimigratory activity of our compounds, we conducted a wound-healing assay using the MCF-7 breast cancer cell line. The assay involved incubating the cells in a minimal serum-containing (2%) medium for 24 or 48 hours after creating a wound by removing silicone inserts. Microscope image analysis was employed to measure the reduction in cell-free areas, which served as an indicator of wound closure. Our findings demonstrated a significant decrease in the migratory capacity of cancer cells (Figure 4 and 5). Notably, both compounds exhibited remarkable antimigratory effects at subantiproliferative concentrations (1.5 μM), with **16BABE** demonstrating more pronounced action after 24 hours of incubation.

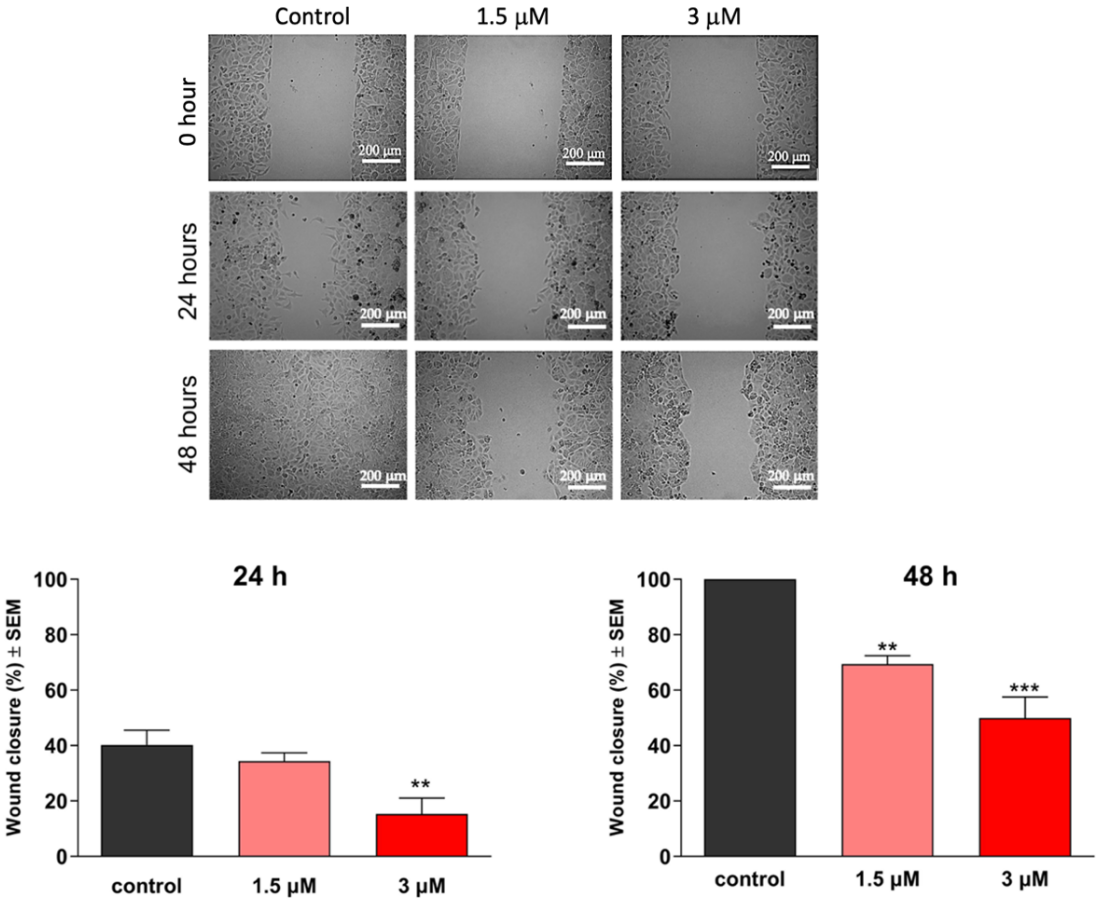

*Figure 4. Effects of 16AABE on the migration of MCF-7 cells. Upper panels: representative images taken at 24 or 48 h post-treatment with 16 16AABE. Lower panels: calculated wound closure values determined after 24 or 48 h post-treatment. ** and *** indicate significance at $p<0.01$ and $p<0.001$, respectively. Findings are based on the results of 4 independent experiments, all performed in triplicate.*

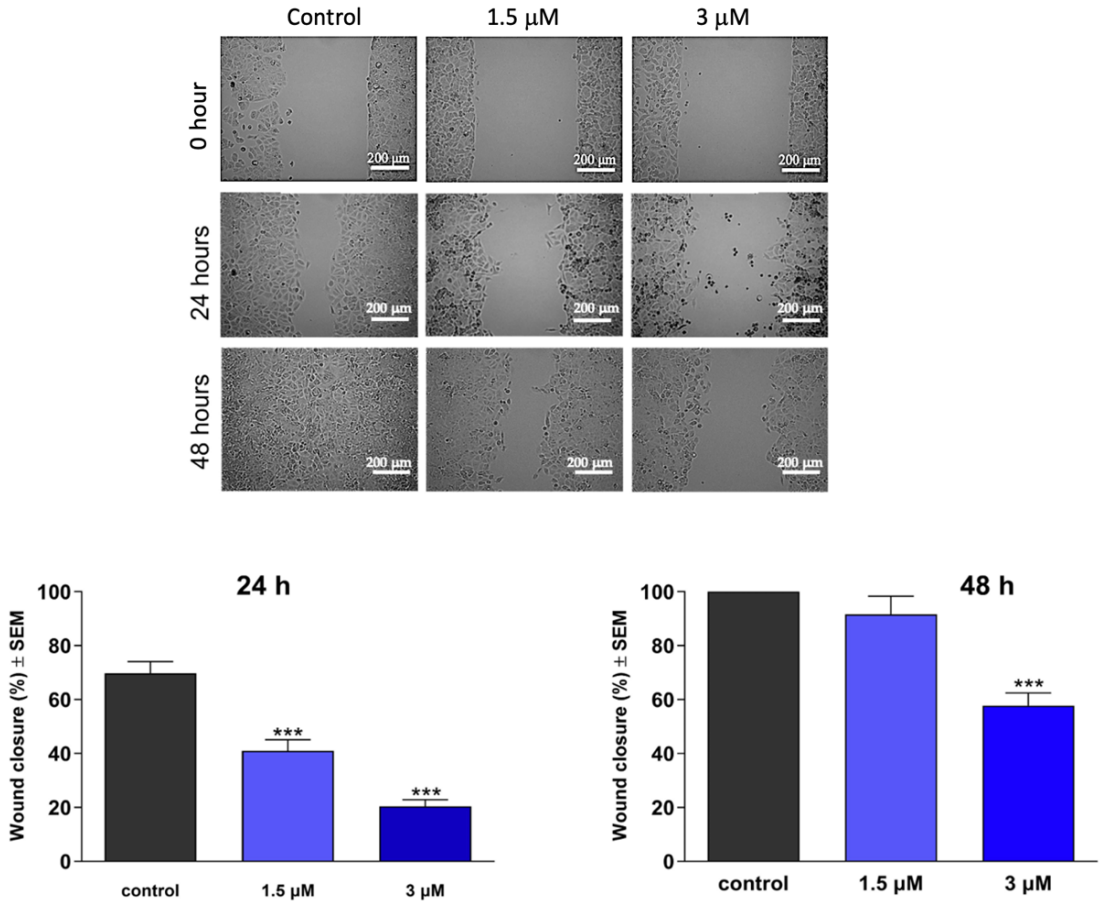

*Figure 5. Effects of 16BABE on the migration of MCF-7 cells. Upper panels: representative images taken at 24 or 48 h post-treatment with 16 16BABE. Lower panels: calculated wound closure values determined after 24 or 48 h post-treatment. *** indicates significance at p<0.001. Findings are based on the results of 4 independent experiments, all performed in triplicate.*

4.5. Boyden Chamber Assay

In addition to its impact on cell migration, the invasive capacity of cancer cells plays a pivotal role in their metastatic behavior, making it a crucial factor in assessing their antimetastatic potential. Boyden chambers with Matrigel Matrix-coated membranes were employed to evaluate invasiveness, as they permit the passage of invasive cells while impeding the migration of non-invading cells. Remarkably, the tested compounds effectively hindered the invasion of MDA-MB-231 cells, even at low concentrations of 0.5 or 1 µM (Figures 6 and 7). Moreover, both compounds exhibited a significant decrease in invading cells after 48 hours of treatment, underscoring their remarkable anti-invasive potential.

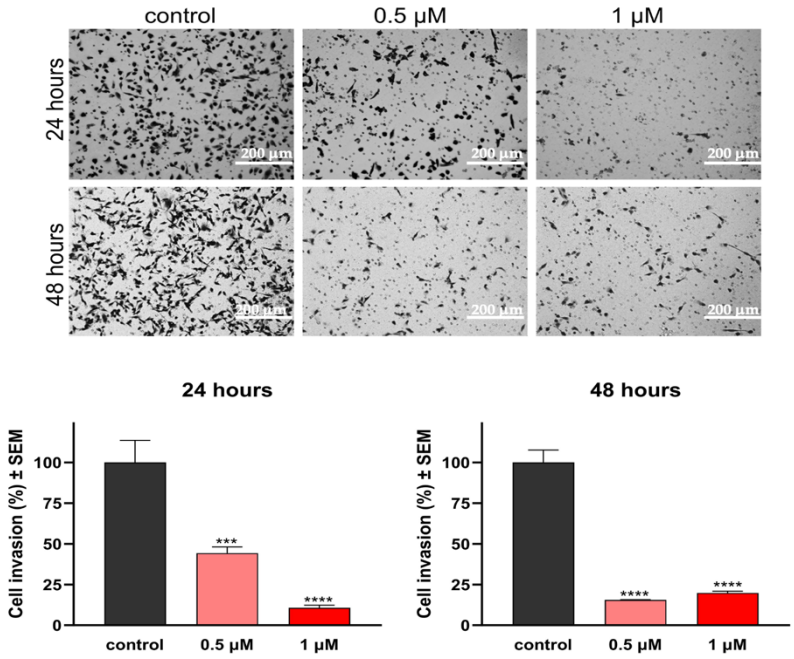

*Figure 6. Effects of 16AABE on the invasion capacity of MBA-MD-231 cells. Upper panels: representative images taken at 24 or 48 h post-treatment with 16AABE. Lower panels: 16AABE significantly reduced invasion of MDA-MB-231 cells at 24-hour and 48-hour treatment. Findings are based on the results of at least 4 independent experiments performed in duplicate. *** and **** indicate significance at p<0.001 and p<0.0001, respectively.*

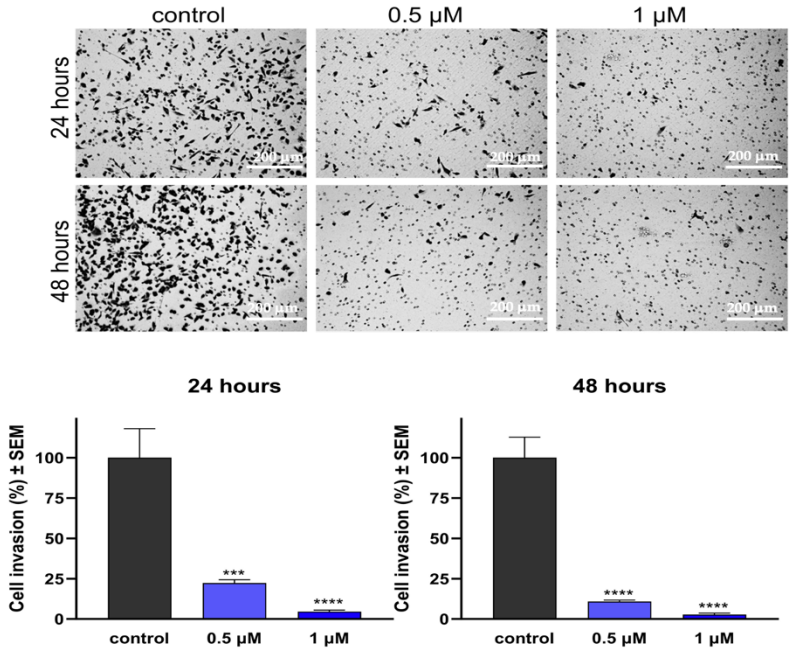

*Figure 7. Effects of 16BABE on the invasion capacity of MBA-MD-231 cells. Upper panels: representative images taken at 24 or 48 h post-treatment with 16BABE. Lower panels: 16BABE significantly reduced invasion of MDA-MB-231 cells at 24-hour and 48-hour treatment. Findings are based on the results of at least 4 independent experiments performed in duplicate. *** and **** indicate significance at p<0.001 and p<0.0001, respectively.*

4.6. Estrogenic Activities of The Tested Compounds

Since the test compounds are structurally closely related to natural estrogen 17β-estradiol, their hormonal activities are considered crucial elements of their pharmacological profile. A T47D breast cancer cell line transfected with an estrogen-responsive luciferase reporter gene was utilized to clarify the estrogenic activity of the tested compounds (Figure 8). Treatment with both compounds resulted in estrogenic activity at concentrations several orders of magnitude higher than reference agents 17β-estradiol. The calculated concentrations eliciting 50% of maximum estrogenic stimulation were approximately 5.5 and 178 nM, respectively. These results indicate that these estrone analogs possess considerable hormonal activity at their antiproliferative or antimetastatic concentrations.

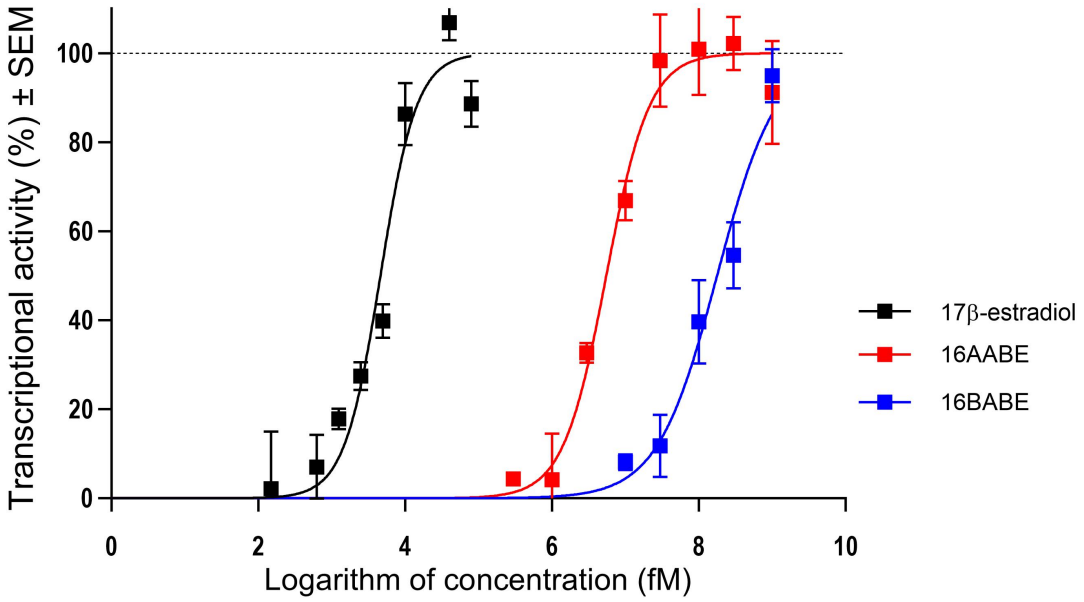

Figure 8. Estrogenic effects of 16AABE and 16BABE expressed as the intensity of the estrogen-responsive luciferase in transfected T47D breast cancer cell line. Findings are based on the results of 3 independent experiments performed in triplicate.

5. Discussion

Breast cancer stands as a complex and intriguing disease, occupying a prominent position as the most frequently diagnosed malignancy among women on a global scale. Its emergence is far from singular, representing a convergence of diverse genetic and environmental factors that complexly shape its pathogenesis. This complex interplay of elements underscores the intricate origins of the disease, underscoring the imperative for a complete comprehension of the underlying mechanisms. In this intricate web of factors, age emerges as a significant player, where both young and older individuals find themselves susceptible. Additionally, the influence of familial history reveals large, amplifying risk. Hormones, the orchestrators of physiological processes, come into play, threading through the intricate narrative of breast cancer's development. Yet, it's not just biology that weaves this story; lifestyle choices, such as dietary habits and exercise routines, interconnect with the genetic. A fundamental framework for deciphering breast cancer's heterogeneity hinges on the molecular classification system. Estrogen and progestin receptors, in tandem with the HER2 status, mark pivotal subtypes of the disease. Through this categorization, the landscape of breast cancer gains a semblance of order, allowing researchers and clinicians to navigate its complicated presentations.

Triple-negative breast cancer (TNBC), with its increased prevalence in younger patients, introduces a unique twist. Accounting for a notable percentage of cases, TNBC presents distinct challenges due to its aggressive behavior and lack of specific molecular targets. This, in turn, calls for innovative therapeutic strategies, pushing the envelope of research and treatment modalities. However, what further enriches the tapestry of breast cancer research is the discovery that certain estrane-based molecules hold potential as potent anticancer candidates. This revelation disrupts conventional assumptions, highlighting the intricate nature of molecular interactions. These compounds, known as 16-substituted triazolyl estranes, showcase remarkable antiproliferative properties, echoing the actions of well-established references like cisplatin. Their impact resonates beyond cell growth inhibition, encompassing cell cycle disruptions and interaction with tubulin protein. A deeper dive into metastasis, the intricate dance of cancer cells spreading to distant sites, unfolds. Metastasis, a hallmark of cancer progression, adds complexity to the equation. A significant challenge in managing breast cancer lies in tackling its metastatic cascade, entailing various stages from local migration to establishment in distant organs. These

multifaceted stages collectively wield a potent influence on cancer prognosis and patient outcomes. In the realm of drug development, 16-substituted triazolyl estranes, specifically **16AABE** and **16BABE**, exhibit significant potential. Their ability isn't confined to mere antiproliferative effects; they display remarkable antimetastatic attributes. This ability to limit cell migration and invasion underscores their potential as candidates for addressing the challenging aspect of metastasis, a crucial battleground in the fight against cancer. While their estrogenic effects raise intriguing possibilities, they also raise caution flags, as hormonal actions can either fuel or reduce cancer growth, depending on the context.

Nevertheless, a theoretical scenario exists wherein a subset of hormone-independent malignancies, such as triple-negative breast cancer, might remain unaffected by the hormonal agonist action. This would imply that the hormonal aspect does not impede the utility of such agents in these specific cancer types. Consequently, the estrone analogs we have presented here hold promise as innovative drug candidates for cancerous disorders that are not influenced by hormonal effects, offering a potentially magnificent way of treatment for these hormone-neutral malignancies. This intriguing prospect underscores the need for nuanced approaches considering the complex interplay between hormonal actions and cancer progression.

PUBLICATIONS RELATED TO THE SUBJECT OF THE THESIS

I. **Senobar Tahaei SA**, Kulmány Á, Minorics R, Kiss A, Szabó Z, Germán P, Szebeni GJ., Gémes N, Mernyák E, Zupkó I: Antiproliferative and antimetastatic properties of 16-azidomethyl substituted 3-*O*-benzyl estrone analogs.
Int J Mol Sci, 2023; 24, 13749

IF: 5.600 / Q1 doi: 10.3390/ijms241813749

II. Jójárt R, **Senobar Tahaei A**, Trungel-Nagy P, Kele Z, Minorics R, Paragi G, Zupkó I, Mernyák E: Synthesis and evaluation of anticancer activities of 2- or 4-substituted 3-(*N*-benzyltriazolylmethyl)-13α-oestrone derivatives.
J Enzyme Inhib Med Chem, 2021; 36: 58-67
IF: 5.756 / Q1 doi: 10.1080/14756366.2020.1838500

III. Kiss A, Wölfling J, Mernyák E, Frank É, Benke Z, **Senobar Tahaei A**, Zupkó I, Mahó S, Schneider G: Stereocontrolled synthesis of the four possible 3-methoxy and 3-benzyloxy-16-triazolyl-methyl-estra-17-ol hybrids and their antiproliferative activities
Steoroids, 2019; 152: 108500
IF: 1.948 / Q2 doi: 10.1016/j.steroids.2019.108500

ADDITIONAL PUBLICATIONS

1. Bamou FZ, Le TM, Tayeb BA, **Tahaei SAS**, Minorics R, Zupkó I, Szakonyi Z: Antiproliferative activity of (−)-isopulegol-based 1,3-oxazine, 1,3-thiazine and 2,4-diaminopyrimidine derivatives. ChemistryOpen 11: e202200169 (2022)
   IF: 2.630 / Q2 doi: 10.1002/open.202200169

2. **Senobar Tahaei SA**, Stájer A, Barrak I, Ostorházi E, Szabó D, Gajdács M: Correlation Between Biofilm-Formation and the Antibiotic Resistant Phenotype in *Staphylococcus aureus* Isolates: A Laboratory-Based Study in Hungary and a Review of the Literature. Infect Drug Resist. 23; 14:1155-1168 (2021)
   IF: 4.177 / Q1 doi: 10.2147/IDR.S303992

3. Csupor D, Kurtán T, Vollár M, Kúsz N, Kövér KE, Mándi A, Szűcs P, Marschall M, **Senobar Tahaei SA**, Zupkó I, Hohmann J: Pigments of the moss Paraleucobryum longifolium: Isolation and structure elucidation of prenyl-substituted 8,8'-linked 9,10-phenanthrenequinone dimers. J Nat Prod 83: 268-76 (2020)
   IF: 4.050 / Q1 doi: 10.1021/acs.jnatprod.0c00243

4. Bús C, Kúsz N, Jakab G, **Senobar Tahaei SA**, Zupkó I, Endrész V, Bogdanov A, Burián K, Csupor-Löffler B, Hohmann J, Vasas A: Phenanthrenes from Juncus compressus Jacq. with promising antiproliferative and anti-HSV-2 activities. Molecules 23: 2085 (2018)
   IF: 3.060 / Q1 doi: 10.3390/molecules23082085